Original article

Evaluation of betanin-encapsulated biopolymeric nanoparticles for antitumor activity via PI3K/Akt/mTOR signaling pathway

Zartasha Rehman [a], Mariam Naveed [b], Bushra Ijaz [b], Muhammad Musaddiq Shah [c], Imran Shahid [d], Mohammad Tarique Imam [e], Ziyad Saeed Almalki [e], Sidra Rehman [a,*]

[a] Department of Biosciences, COMSATS University Islamabad (CUI) Park Road, Islamabad 45550, Pakistan
[b] Centre of Excellence in Molecular Biology (CEMB), University of the Punjab, Lahore 53700, Pakistan
[c] Department of Biotechnology, University of Sialkot, Sialkot, 51040 Pakistan
[d] Department of Pharmacology and Toxicology, Faculty of Medicine, Umm Al-Qura University, Al-Abidiyah, P.O.Box 13578, Makkah 21955, Saudi Arabia
[e] Department of Clinical Pharmacy, College of Pharmacy, Prince Sattam Bin Abdulaziz University, Al Kharj Pin-11942, Saudi Arabia

ARTICLE INFO

ABSTRACT

Cancer nanotheranostic components are useful in monitoring drug delivery and potency against tumor cells. Current chemotherapeutic agents exhibit severe side effects and requires the urgency for discovery of potent therapeutic nano-drugs. So, this study focuses on evaluating the antitumor activity of chitosan nanoparticles encapsulating betanin (CSNPs-BET) against breast cancer (MDA-MB-231) cells. CSNPs-BET were prepared using the ionic gelation method and characterized for their size, polydispersity index (PDI), zeta potential, and surface morphology. Antitumor activity of CSNPs-BET and standard drug, doxorubicin (DOX), was evaluated using MTT, cell migration and gene expression assays. The entrapment efficiency of CSNPs-BET was in the approximate range of 88–91%. The sustained in vitro betanin release pattern was observed under different conditions. Chitosan nanoparticles encapsulated with and without betanin reduced the cell viability in MDA-MB-231 cells with IC$_{50}$ values of 3.974 μg/mL and 7.994 μg/mL, respectively. Further, the treatment of MDA-MB-231 with CSNPs-BET with different concentrations significantly reduced the levels of PI3K (**$P = 0.0016$), Akt (**$P = 0.0014$) and mTOR (****$P < 0.0001$) as compared to control. Inhibition of PI3K and downstream molecules Akt and mTOR by CSNPs-BET resulted in cell proliferation inhibition and cell cycle arrest. Furthermore, CSNPs-BET treated MDA-MB-231 cells probed the significant two-dimensional migration of cells vs. control. Our study findings suggest that nano-scale formulation can improve systematic toxicity and cell proliferation inhibitory activity against cancer cells. In conclusion, the CSNPs-BET improved MDA-MB-231 cells death and depicts promising nano-therapy for breast cancer.

1. Introduction

Cancer, the leading cause of mortality, is reported to have more than 10 million deaths worldwide in 2020 (Sung et al., 2021; Ferlay et al., 2021). Globally, 2.3 million people were affected with breast cancer in 2020, including 0.685 million casualties (Lei et al., 2021). According to the International Agency for Research on Cancer (IARC), in Pakistan, the proportion of newly diagnosed cancer and its relevant mortality cases is 0.18 and 0.11 million, respectively, with a prevalence rate (5 years) of 0.32 million (Hussain et al., 2021). In Pakistan, the breast cancer mortality rate is the topmost globally, with one out of nine women having a lifetime risk of getting the disease (Sarwar and Saqib, 2017). One of the most affected signaling pathways causing breast cellular proliferation, survival and migration includes the PI3K/AKT/mTOR signaling cascade. This signaling pathway plays a major role in cell survival, cell growth, metabolic autophagy programming, transcription regulation and angiogenesis (Ghoneum and Said, 2019). Activated PI3K signaling pathway triggers Protein Kinase B (PKB) activation which phospho-

Production and hosting by Elsevier

rylates other intracellular proteins leading to activation of cell proliferation, cell cycle regulation, apoptosis and DNA repairing mechanisms (Akinleye et al., 2013). Therefore, PI3K/AKT/mTOR signaling pathway represents one of the most effective drug targets (Gohr et al., 2017).

Unfortunately, conventional chemotherapeutics lack their selectivity, oral bioavailability, and specificity, that often resulting in adverse side effects (Loerzel, 2015). Drug nano-scale formulations have gained extensive interest in cancer therapeutics due to their stability, size, specificity, and other tunable characteristics. Among various nanocarrier systems, polymeric nanoparticles are the most widely employed form of nanoparticles used for analysis of anti-cancer activity (Tran et al., 2020). Previous studies reported that polymeric nanoparticles can increase the bioavailability of loaded phytochemical compounds and are potentially safe for human usage (Sartaj et al., 2021; Sakhi et al., 2022; Xiong et al., 2020). Biopolymeric nanoparticles that are used in food and pharmaceutical industries for delivering drugs might enhance their therapeutic efficacies against cancer (Udayakumar et al., 2021; Baranwal et al., 2022; Hosseini et al., 2022). Additionally, chitosan has very low toxicity for other fibroblast cells; its cationic properties and electrostatic attraction have drawn attention towards its therapeutic potential. Chitosan nanoparticles (CSNPs) have good bioavailability, biocompatibility, biodegradability, adsorption, loading capacity; therefore, can be used as cancer drug carriers (Wu et al., 2019; Shafqat et al., 2023).

Betalains are nitrogen-containing hydrophilic compounds mainly divided into two groups: betacyanins and betaxanthins. Betanin (betanidin-5-O-β-glucoside) is a natural red food colorant and the only phytoconstituent of betacyanins approved for use in the cosmetic, pharmaceutical, and food industries (Shafqat et al., 2023). Betanin is usually well-tolerated and safe, but its stability and bioavailability, however, need to be improved. Therefore, nanoformulations can be an alternative to address this health issue. For this purpose, this study focused on the evaluation of nano formulations using hydrophilic drugs against breast cancer cells.

Considering the therapeutic potency of betanin and chitosan bioactive polymer, herein, we reported the evaluation of antitumor activity of CSNPs-BET against breast cancer cells. Likewise, it is worth specifying here that this is the first study to evaluate the antitumor activity of betanin-encapsulated chitosan nanoparticles in MDA-MB-231 cells.

2. Materials and methods

2.1. Materials

Chitosan was purchased from Solar Bio (Medium molecular weight (MW), deacetylation degree < 90 %). Betanin (BET) (B0397) was purchased from Tokyo Chemical Industry (TCI) Co., LTD, Japan. Sodium Tripolyphosphate (TPP), acetic acid (CH_3-COOH), sodium hydroxide pellets (NaOH), hydrochloric acid, ethanol, and dimethyl sulfoxide (CAS/CAT no. (67–68-5) was purchased from Roth Industries, Germany. Ultrapure deionized water (Invitrogen) was used for dilution throughout this experiment.

2.2. Biosynthesis and physicochemical characterization of chitosan nanoparticles

CSNPs-BET and chitosan nanoparticles without BET (CSNPs) were prepared using the ionic gelation method reported in our previous work (Shafqat et al., 2023). Precisely, chitosan (0.3 g) was added to 1% acetic acid solution and poured into the deionized water to make a solution of 100 mL. Betanin (8.0 mg) was dissolved

in DMSO (1 mL) and progressively added to the chitosan solution. At room temperature, this solution was left over for 24 h on a magnetic stirrer (600 rpm). After that time, the pH of the solution was adjusted to 4.8. Trisodium polyphosphate (TPP, 0.1 %) was prepared in ultra-pure water and added dropwise to the chitosan solution mixture. The mixture was kept on continuous stirring for 2 h till the formation of an opalescent suspension. The suspension analysis was performed on a prob sonicator for 60 mins of 20 secs on and 10 mins off cycle on ice bath. Different characterization techniques were performed to determine the surface charge, diameter and size distribution, and polydispersity index value of these CSNPs-BET (Xu et al., 2022).

2.3. Analysis of drug encapsulation and in vitro release pattern of betanin

The drug encapsulation efficacy of CSNPs-BET was evaluated using a UV–Vis spectrophotometer. Briefly, multiple serial dilutions of betanin samples were taken, and a standard curve was The in vitro release pattern of betanin from chitosan nanoparticles at two different pH values was determined following the protocol used in our previous study (Shafqat et al., 2023).

2.4. Cell culture and formazan-based MTT assay

MDA-MB-231 breast cancer cells were cultured in high glucose concentration with a density of $4x10^4$ cells. Cells were grown in the presence of 12% fetal bovine serum (FBS), 100 IU mL^{-1} penicillin, and 100 μg mL^{-1} streptomycin. Cells were incubated at 37 °C for 24 h with 5% CO_2 in a humidified incubator. For analysis of cell proliferation inhibition activity, MDA-MB-231 cells were grown at a density of $4x10^4$ cells per well in 96 wells plates according to our previously described protocol (Rehman et al., 2011). BET-CSNPs were added in serial dilutions (2.5–80 μg/mL) to the cultured cells with a 70–75% confluency. After 24 h of incubation, MTT solution was added to each well, and cells were incubated at 37 °C for 3–4 h. The absorbance of formazan crystals (dissolved in organic solvent) was measured at 570 nm with a reference wavelength of 620 nm. Doxorubicin (DOX) was used as a positive control. IC$_{50}$ values were calculated by plotting a linear regression curve using the log concentrations of samples versus normalized % cell viability inhibition.

2.5. Migration assay

For analysis of cell movement in controlled in vitro conditions, migration assay was performed with some modifications previously described by Zhu et al. (Zhu et al., 2013). Briefly, 5×10^5 cells were seeded to a 12-well plate and incubated for 24 h with 5% CO_2 concentration at 37 °C. Followed by incubation, media was removed from wells, and cells were washed with 1X PBS. A monolayer of cells was scratched to form a fixed-width line and a cross-shaped wound in all wells. Followed by cell scratching, they were treated with effective concentrations (5 μg/ml and 20 μg/ml) of CSNPs-BET and DOX along with negative control. Cell migration assay was evaluated based on the wound-healing process.

2.6. Gene expression analysis

Real-time Polymerase Chain Reaction (RT-PCR) technology has significantly changed the field of analyzing gene expression. The beneficial effect of phytochemicals for reducing the level of tumor-promoting gene expression in malignant breast cell types can be improved by loading them into chitosan nanoparticles. For analysis of the CSNPs-BET effect on PI3K/AKT/mTOR pathway in MDA-MB-231 cells, RT-PCR was performed (Chen et al., 2021).

Briefly, RNA was extracted from treated MDA-MB-231 cells using TRIzol reagent (Invitrogen, USA). RNA purification and quantification were determined by Nanodrop (ND-1000, Optiplex, USA). cDNA was prepared from 1 µg RNA using RevertAid First Strand cDNA synthesis kit (Thermo Scientific, USA). RT-PCR was performed using SYBR Green master mix (Thermo Scientific, USA) under these conditions: 50 °C for 2 mins, 95 °C for 10 mins, and 40 cycles of 95 °C for 15 s and 58 °C for 30 s and 60 °C for 60 s using GAPDH (internal control) and genes specific primers (Table 1). A melting curve was generated for the confirmation of amplification specificity. GAPDH was taken as an internal control, and the qPCR reaction was repeated in triplicates. The formula $^\Delta$Ct = Ct gene -Ct reference was applied to represent the relative gene expression level. Gene expression fold change was calculated through the $2^{-\Delta\Delta Ct}$ method. Data acquisition was carried out during the extension step of qPCR.

2.7. Statistical analysis

The statistical analysis of data was expressed in mean standard deviation ± of readings. Wound healing is calculated as a proportion of the total control migration observed. Graphs were plotted by using GraphPad Prism software and Origin Pro-2018. IC_{50} values of MTT assays were calculated to find the cell viability of the encapsulated drug for antitumor activity. The analysis of variance (ANOVA) was used to analyze the data and determine the value of the samples at the level of $P < 0.05$, statistically significant.

3. Results and discussion

3.1. Assessment of CSNPs-BET characteristics using UV, FTIR, DLS, and SEM

The hydrodynamic particle size of CSNPs-BET with zeta potential, PDI measurement, encapsulation efficiency, and % release value of betanin from chitosan nanoparticles is given in Table 2. Nanoparticles are biologically adaptable due to their small size concerning rapid renal discharge while keeping a deliberate distance from components of the reticular endothelial system. In such a manner, nanotheranostic materials for cancer treatment is encouraged due to their enhanced penetration, drug aggregation, and retention impact in tumor cell after endocytosis (Naahidi et al., 2013). In our study, nanoparticles with a size of 270.8 ± 8.1 0 nm using zeta-sizer (Nanotrac Wave-II) were synthesized, and this small size may enhance blood flow time and directly target tumors, according to the previous study reported by Wang et al. (Wang et al., 2015). FTIR (FTIR- 8400 spectrophotometer) assessed specific interactions of functional groups with chitosan nanoparticles. Optical properties of CSNPs-BET were studied using UV–Vis spectrophotometer (HITACHI U-2900), and a broad curve was observed at 310 nm (Fig. 1b). Surface morphology of nanoparticles was determined by SEM, revealing that CSNPs-BET is nanospherical in shape with a smooth surface (Fig. 1d). Prasad et al. (Prasad et al., 2022) also observed the smooth spherical shape of

Table 1
Primer sequences of genes used in RT-PCR.

Genes		Sequences	Annealing temp.
PI3K	F	5-CCCGTGGTTATGAATGTGCT-3	58 °C
	R	5-AAATGGTAGCTTCCCGAGGT-3	
mTOR	F	5-CACCCGAATTGGCAGATTT-3	59 °C
	R	5-GCTCGCTTCACCTCAAATTC-3	
AKT	F	5-TACCCAGTGGGACAGAGGAG-3	59 °C
	R	5-AGCGTCGAAAAGGTCAAGTG-3	
GAPDH	F	5-GGATTTGGTCGTATTGGG-3	58 °C
	R	5-GGAAGATGGTGATGGGATT-3	

chitosan nanoparticles with the size of 160 nm. Wu et al. (Wu et al., 2018) made formulations of *Torreya grandis* aril essential oils loaded in chitosan nanoparticles with the dimensions of 349.6 ± 1 0.55 and 542.9 ± 16.74 nm with spherical structure. Ganesan et al. (Ganesan et al., 2022) synthesized salsalate-loaded chitosan nanoparticles with a size of 132.8 ± 17.4 nm having a spherical surface.

3.2. Drug release profiling for CSNPs-BET

In the *in vitro* drug release assay, a burst release of betanin was noted for the first 2.0 h, followed by a sustained release pattern at both pH (pH: 4.0, pH:7.4) (Fig. 1c). At pH 4.0, 74 % of the drug was released while at pH 7.4, 86% of the drug was released (Table 2). For analysis of drug release profile, sudden bursts and sustained release patterns are studied. Surface assimilation of the drug on nanoparticles resulted in the initial swift burst phase. In comparison, a moderate dispersal of the drug from nanocarrier system and the subsequent disintegration of polymeric matrix is responsible for the sustained release of drug (Arafa et al., 2020). The *in vitro* release study of BET from CSNPs using phosphate buffered saline at two different pH (7.4, 4.0) for 72 h was conducted. The released percentage was estimated considering the encapsulated BET concentration. Initially, there was an initial burst release of BET (67% at pH 4.0; 78.6%) at 2.0 h followed by a slow release from 2 to 48 h when almost 74% and 86% of the BET was released, as shown in Fig. 1c. The burst release might be due to the surface assimilation of BET with poor entrapment in polymer of CSNPs and moderate release is due to the diffusion of BET drug found in the core of nanoparticles. Prolonged release of BET by CSNPs was observed and a detailed drug release kinetics study was discussed in our previous study (Shafqat et al., 2023). Our research findings for drug release patterns were found in consistent with the earlier studies (Ganesan et al., 2022; Rozana et al., (2020)). Based on previous study results, it may be likely to develop CSNPs-BET into a potent drug for diseases such as cancer that need controlled drug release in biological systems (Ganesan et al., 2022).

3.3. CSNPs-BET inhibited cellular proliferation

The anticancer effect of CSNPs-BET against MDA-MB-231 cells was investigated using a conventional MTT assay. The MTT assay depicted the percent viability of MDA-MB-231 cells at different concentrations of drugs. In our study, MDA-MB-231 cells were treated with multiple serial dilutions (2.5 µg/mL-80 µg/mL) of CSNPs, CSNPs-BET, and DOX. At lower concentrations of DOX, i.e., 2.5 and 5.0 µg/mL, cells are significantly viable, while at higher concentrations, i.e., 40 and 80 µg/mL, the percent cell viability was 20.5 and 25.3%, respectively (Fig. 2a). Conversely, for cells treated with lower concentrations of CSNPs-BET i.e., 2.5 and 5.0 µg/mL, the percent cell viability was 67 and 69.2% respectively (Fig. 2a). This showed that 2.5 µg/mL formulations of CSNPs-BET were effective than others. In a previous study by Prasad et al., the percent cell viability of curcumin-loaded chitosan nanoparticles in Vero cells was analyzed at different concentrations (10, 20, 50 µg). The nanoparticles exhibited the lowest cell viability (76% ± 29) at 50 µg (Prasad et al., 2022). Kumar et al. (Kumar et al., 2018) fabricated vincristine-loaded chitosan nanoparticles and found their cytotoxicity against lung cancer cells (NCI-H460) at different concentrations (5, 10, 15, 20, 25 mg/mL). The lowest percent cell viability (32.8%) was observed at 10 mg/mL. In a similar way, Mani et al. (Mani et al., 2020) synthesized proanthocyanidin-chitosan nanoparticles (PAC-CSNPs) to analyze HT-29 cells proliferation inhibition. PAC-CSNPs inhibited (50.83 ± 0.82%) human colorectal carcinoma cells (HT-29) at the low dose concentration of 6.25 µg/mL. Our cytotoxicity results are in corre-

Table 2
Characteristics of CSNPs-BET nanoformulation.

Sample	PDI	Zeta potential	Size	% EE	% Drug release
CSNPs-BET	0.05	+31.3 mV	270.8 ± 8.10 nm	91	74 pH: 4.0 86 pH: 7.4
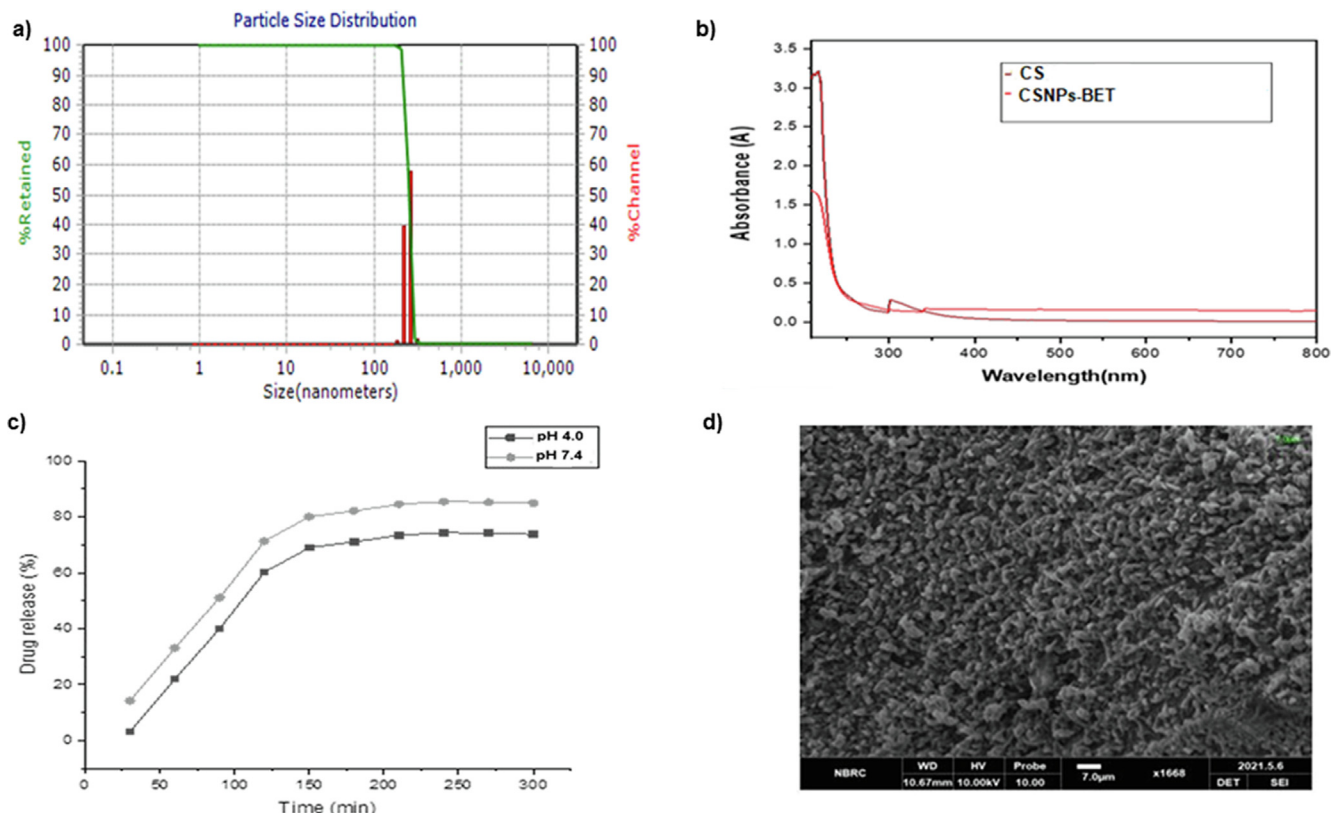
Fig. 1. a) DLS particle size (nm) distribution of CSNPs-BET nanoparticles b) UV-Vis spectrum for analyzing absorbance pattern of Chitosan (CS) and CSNPs-BET c) % drug release pattern analysis from CSNPs-BET nanoparticles d) SEM micrograph with 7.0 μm scale at working distance of 10.61 mm.

lation with these above-reported studies. Another study carried out by Danafar et al. (Danafar et al., 2017) determined the enhanced cell proliferation inhibition effect of sulforaphane (SF) and curcumin (CUR) loaded PEGylated Fe3O4@AuNPs on breast adenocarcinoma cells (SK-BR-3) contrasted to free SF and CUR.

Half-maximal (50%) inhibitory concentration (IC_{50}) was also measured to determine 50% cell viability in MDA-MB-231 cells. Determination of IC_{50} values is crucial for the estimation of biological and pharmacological characteristics of chemotherapeutic drugs (He et al., 2016). In our study, MTT data revealed that CSNPs-BET exhibited the lowest IC_{50} value (3.974 μg/mL) contrasted to blank chitosan nanoparticles (CSNPs) and DOX (7.994 and 9.070 μg/mL, respectively) (Fig. 2b-2d). Lower IC_{50} indicated the potent cytotoxic effect of CSNPs-BET on breast cancer cells. These findings agree with previous studies on natural products against multiple cancer cell lines (Alkahtani et al., 2022). These outcomes revealed that CSNP nanoparticles are notably cytocompatible and can be used as safe antitumor drug carriers (Mani et al., 2020). The current study also confirmed that CSNPs-BET at the lowest concentration (2.5 μg/mL) is therapeutically safe for cellular proliferation inhibition.

### 3.4. Interference of CSNPs-BET with MDA-MB-231 cells' motility

The wound closure assay utilized MDA-MB-231 cells as an *in vitro* model system. In this assay, cell migration activity in

response to mechanical scratch was conducted in the presence and absence of CSNPs-BET and DOX as inhibitors. The percentage of wound area was determined after 24 h for quantifying the effect of migration inhibitor (Fig. 3). Our study data showed that CSNPs-BET at 20 μg/mL inhibited scratch closure (44%) while DOX at 80 μg/mL showed 48% cell migration inhibition (Fig. 3a). Further, results in Fig. 3b revealed that the scratch area was completely closed after 48 h of treatment of CSNPs-BET and DOX. In cancer research, cell migratory activity can be measured in immunological, developmental, and wound/scratch healing studies. *In vitro* wound closure assay depicts the cells' mobility behavior (Castellone et al., 2011). Our study used this cell motility assay to determine the migration activity of MDA-MB-231 cells in a time-dependent manner. The *in vitro* cell scratch closure assay investigates a particular cell line behavior towards migration, and afterward, complete wound closure was observed in the confluent layer of cells. This primary *in vitro* cell migration assay is readily accessible for researchers with essential equipment and is relatively simple in performance (Justus et al., 2014; Pijuan et al., 2019).

The molecular functioning of all the significant pathways of wound healing in cancer depicts their seminal association (Dvorak, 2015). A study conducted by Stuelten et al. revealed that wound microenvironment is a contributive factor for cancer progression (Stuelten et al., 2008). Wound healing and cancer are remarkably complex processes; both occur due to the coordinated
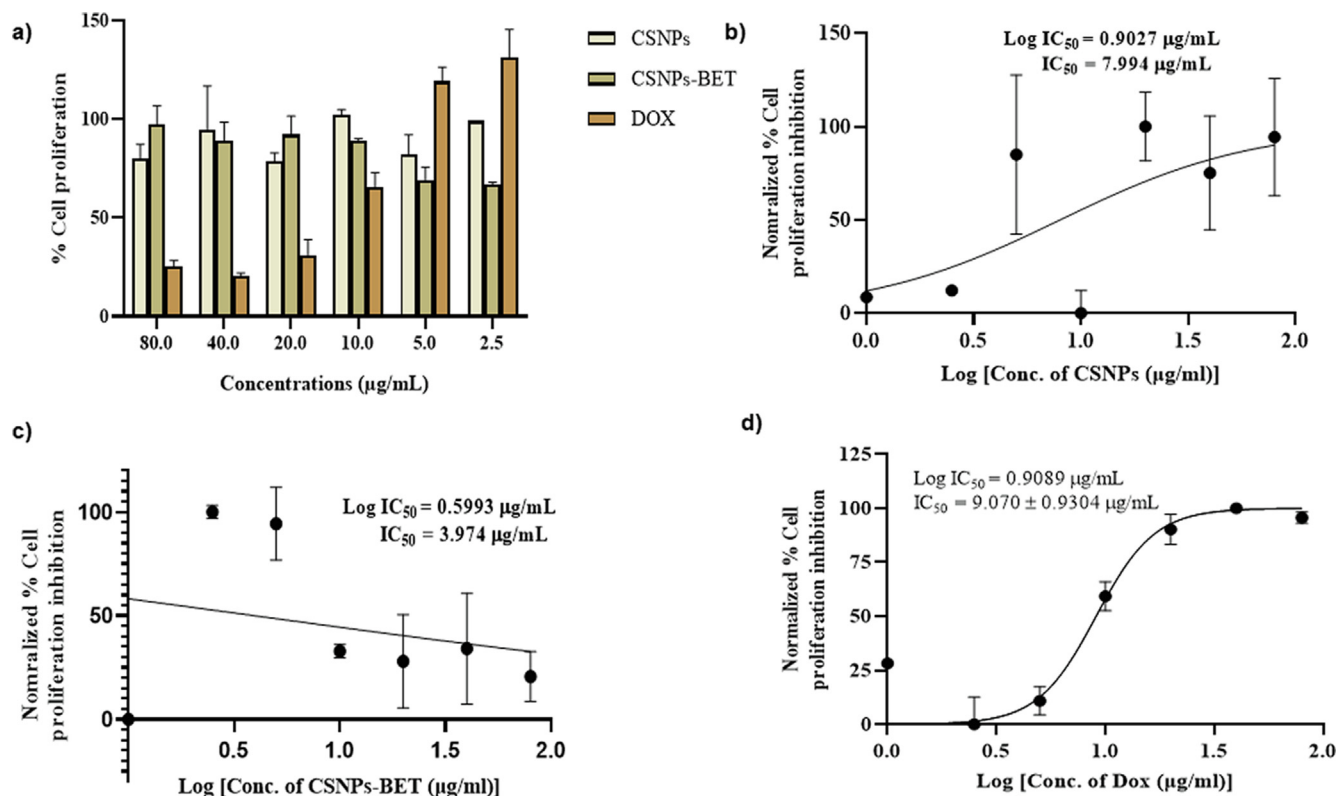
Fig. 2. a) Cell proliferation analysis of synthesized CSNPs-BET nanoparticles, CSNPs without drug and doxorubicin (DOX) on MDA-MB-231 cells b) IC_{50} value analyzed from normalized % cell proliferation inhibition pattern by CSNPs without drug c) IC_{50} value for cell proliferation inhibition by CSNPs-BET d) IC_{50} value for MDA-MB-231 cells proliferation inhibition by DOX.
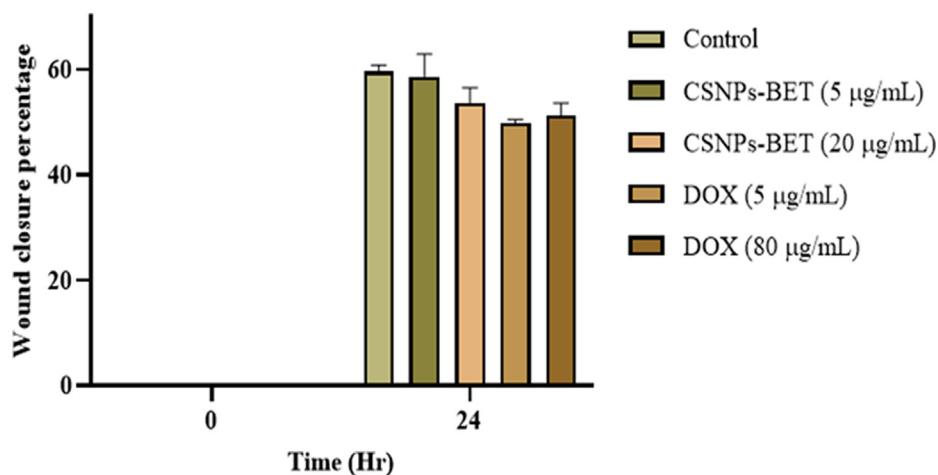

Fig. 3. The effect of CSNPs-BET and DOX on MDA-MB-231 cells migratory activity at different concentrations.

functioning of migration and proliferation. These migratory and proliferative behaviors of cells have resulted from interactions among different types of cells, such as mesenchymal, endothelial, epithelial, and immune cells, via cytokines/growth factors signaling pathways. For example, in the case of re-epithelialization, keratinocytes migrate over the scratch bed due to both intracellular processes, such as cytoskeletal rearrangement, and extracellular mechanisms, such as cell-matrix and cell–cell interactions, membrane remodeling, and proteinase-assisted matrix modification. Most of these processes also work during cancer development and progression, such as promigratory proteins are required for both keratinocyte migration and epithelial cancers (Abreu-Blanco

et al., 2012; Hopkinson et al., 2014; Caley et al., 2015; Sundaram et al., 2017).

3.5. CSNPs-BET causes a significant decrease in PI3K/Akt/mTOR expressions in MDA-MB-231 cells

The PI3K/Akt/mTOR signaling pathway significantly contributes to cancer cell growth, proliferation, metastasis, cell cycle, apoptosis, and autophagy (Alzahrani, 2019; Pompura and Dominguez-Villar, 2018; Li et al., 2021). Treatment of MDA-MB-231 cells with CSNPs-BET at two different concentrations (5 μg/mL & 20 μg/mL) manifested a significant ($P < 0.05$) decrease in the expression of
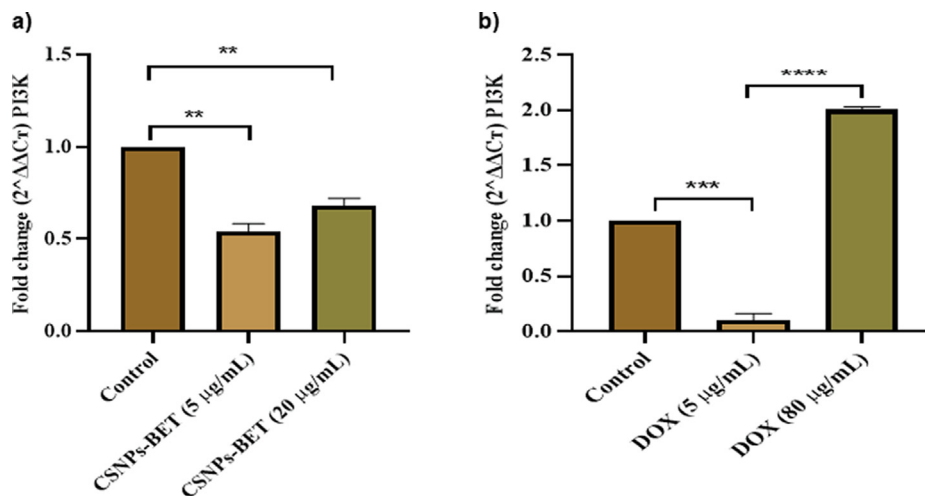
Fig. 4. a) Real time PCR results show that CSNPs-BET has reduced the mRNA expression of PI3K at lower dose of 5 μg/mL b) The graphical illustration for real time PCR results shows that DOX at 5 μg/mL inhibited PI3K mRNA expression level significantly. The error bars represent the mean ± standard deviation of triplicate results. $^*P < 0.05$, $^{**}P < 0.01$, $^{***}P < 0.001$ vs. control.
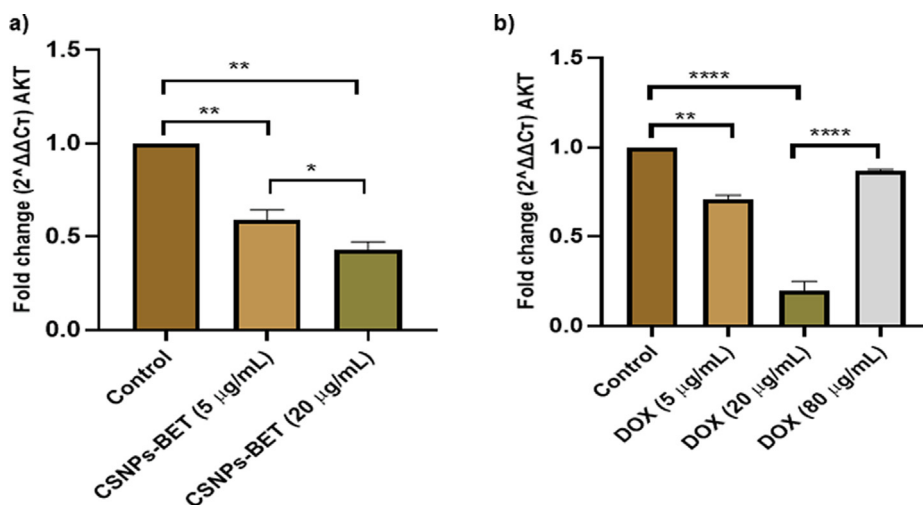
Fig. 5. Reduced Akt expression in MDA-MB-231 cells after treatment with different concentrations of a) Synthesized CSNPs-BET b) Doxorubicin (DOX). $P < 0.05$, $^{**}P < 0.01$, $^{***}P < 0.001$ vs. control.

PI3k, Akt, and mTOR signaling pathways as compared to control. Fig. 4a and 5a illustrate that compared with the control group, gene expression of PI3K and Akt decreased after 24 h of treatment with CSNPs-BET. In addition, we found that CSNPs-BET treatment of MDA-MB-231 cells inhibited the gene expression level of mTOR (Fig. 6a). Based on these study data, we hypothesized that CSNPs-BET suppressed the PI3K/Akt/mTOR pathway. Furthermore, we have found the significant ($P < 0.05$) inhibition of gene expression in PI3K/Akt/mTOR signaling pathway when treated cells with DOX mainly at two different concentrations (5 and 20 μg/mL) after 24 h of treatment (Fig. 4b, 5b & 6b). However, DOX at a higher concentration (80 μg/mL) did not show inhibition of this pathway.

A study conducted by Badawy et al. revealed that administering the chitosan-coated iron oxide nanoparticles significantly inhibited PI3K/Akt/mTOR pathway gene expressions in rat liver cancer cells (Badawy et al., 2023). Another study performed by Subramaniyan et al. found that zinc oxide nanoparticles stabilized by *Solanum xanthocarpum* extract inhibited the PI3K/Akt/mTOR pathway and upregulated the beclin-1 and LC3 expression in osteosarcoma MG63 cells (Subramaniyan et al., 2022). Our study results align with the previous studies indicating that suppression of PI3K/

Akt/mTOR signaling pathway can lead to apoptosis and cancer cell death.

The PI3K/Akt/mTOR signaling pathway is a complex intracellular signaling pathway that is a significant regulatory contributor in cell cycle control and is most commonly impaired in cancer (Patnaik et al., 2011). Many cancer biology studies reported a 50–70% increase in Akt expression due to PI3K/AkT/mTOR signaling (Yip, 2015). PI3K phosphorylation triggers AkT, which modulates multiple downstream molecules, including mTOR. In many cancers, such as hepatocellular carcinoma and breast cancer, the PI3K/AkT/mTOR signaling pathway is hyperactive, decreasing apoptotic and increasing cellular proliferative activity (Vij and Calderaro, 2021; Sandhiutami et al., 2021). It is revealed that a therapeutic agent that inhibits the overexpression of PI3K/Akt/mTOR molecules can be a potent drug for breast cancer treatment. Therefore, we evaluated the effect of betanin-encapsulated nanoparticles on the suppression of PI3K/Akt/mTOR signaling molecules in MDA-MB-231 cells.

Nanoparticles-based PI3K/Akt/mTOR targeted therapy seems an alternative potent therapeutic option for different malignancies, including breast cancer. It is essential to mention here that many
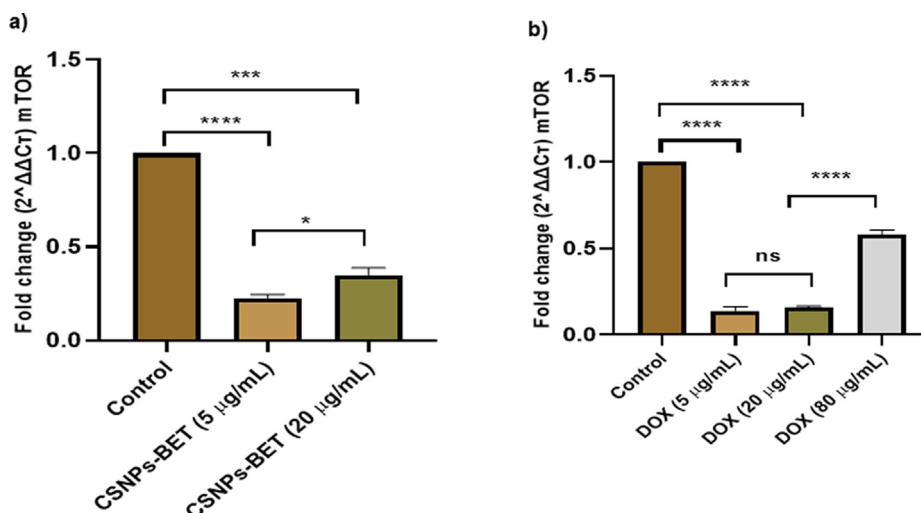
Fig. 6. a) CSNPs–BET treatment to breast cancer cells at different concentrations significantly reduces the mRNA expression of mTOR b) DOX treatment inhibits the gene expression of mTOR in MDA-MB-231 cells. $P < 0.05$, $^{**}P < 0.01$, $^{***}P < 0.001$ vs. control.

studies suggest that various nanoparticles can regulate mTOR activation, resulting in cell cycle arrest in cancer cells (Chiu et al., 2015). Previous studies reported the mTOR phosphorylation (Shen et al., 2020) and Akt (Shetake et al., 2015) inhibition by Fe_3O_4 nanoparticles. The current research has conclusively found the therapeutic role of betanin-encapsulated chitosan nanoparticles as an alternative treatment in breast cancer cells through inhibition of PI3K/Akt/mTOR pathway.

4. Conclusion

In conclusion, the synthesized CSNPs-BET nanoparticles were investigated for the purpose of successful drug delivery. Study results proved that CSNPs-BET enhanced the antitumor activity of betanin in MDA-MB-231 cells with underlying mechanism modifying the PI3K/Akt/mTOR signaling pathway. Furthermore, CSNPs-BET inhibited cellular proliferation and cell migration as an additional effect in protecting the cells from abrupt cellular growth and division. An added effect of delivering betanin in chitosan nanoparticles may be the possibility to enhance the shelf-life of betanin. Conclusively, the current study has proven the advancement of alternative medicine approach for anti-breast cancer.

CRediT authorship contribution statement

Zartasha Rehman: Methodology, Writing – original draft. **Mariam Naveed:** Methodology. **Bushra Ijaz:** Formal analysis, Data curation. **Muhammad Musaddiq Shah:** Writing – review & editing, Resources. **Imran Shahid:** Validation, Software. **Mohammad Tarique Imam:** Resources, Formal analysis. **Ziyad Saeed Almalki:** Software. **Sidra Rehman:** Supervision, Conceptualization, Writing – original draft, Validation.

Declaration of competing interest

The authors declare that they have no known competing financial interests or personal relationships that could have appeared to influence the work reported in this paper.

Funding Statement

References

Abreu-Blanco, M.T., Watts, J.J., Verboon, J.M., Parkhurst, S.M., 2012. Cytoskeleton responses in wound repair. Cell. Mol. Life Sci. 69, 2469–2483.
Akinleye, A., Avvaru, P., Furqan, M., Song, Y., Liu, D., 2013. Phosphatidylinositol 3-kinase (PI3K) inhibitors as cancer therapeutics. J. Hematol. Oncol. 6 (1), 1–17.
Alkahtani, S.A., Alshabi, A.M., Shaikh, I.A., Orabi, M.A., Abdel-Wahab, B.A., Walbi, I.A., et al., 2022. In Vitro Cytotoxicity and Spectral Analysis-Based Phytochemical Profiling of Methanol Extract of Barleria hochstetteri, and Molecular Mechanisms Underlying Its Apoptosis-Inducing Effect on Breast and Lung Cancer Cell Lines. Separations 9 (10), 298.
Alzahrani, A. S. 2019. PI3K/Akt/mTOR inhibitors in cancer: At the bench and bedside. In Seminars in cancer biology (Vol. 59, pp. 125-132). Academic Press.
Arafa, M.G., Mousa, H.A., Afifi, N.N., 2020. Preparation of PLGA-chitosan based nanocarriers for enhancing antibacterial effect of ciprofloxacin in root canal infection. Drug Deliv. 27 (1), 26–39.
Badawy, M.M., Abdel-Hamid, G.R., Mohamed, H.E., 2023. Antitumor Activity of Chitosan-Coated Iron Oxide Nanocomposite Against Hepatocellular Carcinoma in Animal Models. Biol. Trace Elem. Res. 201 (3), 1274–1285.
Baranwal, J., Barse, B., Fais, A., Delogu, G.L., Kumar, A., 2022. Biopolymer: A sustainable material for food and medical applications. Polymers 14 (5), 983.
Caley, M.P., Martins, V.L., O'Toole, E.A., 2015. Metalloproteinases and wound healing. Adv. Wound Care 4 (4), 225–234.
Castellone, R.D., Leffler, N.R., Dong, L., Yang, L.V., 2011. Inhibition of tumor cell migration and metastasis by the proton-sensing GPR4 receptor. Cancer Lett. 312 (2), 197–208.
Chen, H., Feng, X., Gao, L., Mickymaray, S., Paramasivam, A., Abdulaziz Alfaiz, F., et al., 2021. Inhibiting the PI3K/AKT/mTOR signalling pathway with copper oxide nanoparticles from Houttuynia cordata plant: attenuating the proliferation of cervical cancer cells. Artif. Cells Nanomed. Biotechnol. 49 (1), 240–249.
Chiu, H.W., Xia, T., Lee, Y.H., Chen, C.W., Tsai, J.C., Wang, Y.J., 2015. Cationic polystyrene nanospheres induce autophagic cell death through the induction of endoplasmic reticulum stress. Nanoscale 7 (2), 736–746.
Danafar, H., Sharafi, A., Askarlou, S., Manjili, H.K., 2017. Preparation and characterization of PEGylated iron oxide-gold nanoparticles for delivery of sulforaphane and curcumin. Drug research 67 (12), 698–704.
Dvorak, H.F., 2015. Tumors: wounds that do not heal—redux. Cancer Immunol. Res. 3 (1), 1–11.
Ferlay, J., Colombet, M., Soerjomataram, I., Parkin, D.M., Piñeros, M., Znaor, A., Bray, F., 2021. Cancer statistics for the year 2020: An overview. Int. J. Cancer 149 (4), 778–789.
Ganesan, S., Alagarasan, J.K., Sonaimuthu, M., Aruchamy, K., Alkallas, F.H., Ben Gouider Trabelsi, A., et al., 2022. Preparation and Characterization of Salsalate-Loaded Chitosan Nanoparticles. In Vitro Release and Antibacterial and Antibiofilm Activity. Mar. Drugs 20 (12), 733.
Ghoneum, A., Said, N., 2019. PI3K-AKT-mTOR and NFκB pathways in ovarian cancer: implications for targeted therapeutics. Cancers 11 (7), 949.
Gohr, K., Hamacher, A., Engelke, L.H., Kassack, M.U., 2017. Inhibition of PI3K/Akt/mTOR overcomes cisplatin resistance in the triple negative breast cancer cell line HCC38. BMC Cancer 17, 1–13.

He, Y., Zhu, Q., Chen, M., Huang, Q., Wang, W., Li, Q., et al., 2016. The changing 50% inhibitory concentration (IC50) of cisplatin: a pilot study on the artifacts of the MTT assay and the precise measurement of density-dependent chemoresistance in ovarian cancer. Oncotarget 7 (43), 70803.

Hopkinson, S.B., Hamill, K.J., Wu, Y., Eisenberg, J.L., Hiroyasu, S., Jones, J.C., 2014. Focal contact and hemidesmosomal proteins in keratinocyte migration and wound repair. Adv. Wound Care 3 (3), 247–263.

Hosseini, S.F., Ghaderi, J., Gómez-Guillén, M.C., 2022. Tailoring physico-mechanical and antimicrobial/antioxidant properties of biopolymeric films by cinnamaldehyde-loaded chitosan nanoparticles and their application in packaging of fresh rainbow trout fillets. Food Hydrocoll. 124, 107249.

Hussain, I., Majeed, A., Rasool, M.F., Hussain, M., Imran, I., Ullah, M., Ullah, H., 2021. Knowledge, attitude, preventive practices and perceived barriers to screening about colorectal cancer among university students of newly merged district, Kpk, Pakistan–A cross-sectional study. J. Oncol. Pharm. Pract. 27 (2), 359–367.

Justus, C.R., Leffler, N., Ruiz-Echevarria, M., Yang, L.V., 2014. In vitro cell migration and invasion assays. JoVE (Journal of Visualized Experiments) 88, e51046.

Kumar, N., Salar, R.K., Prasad, M., Ranjan, K., 2018. Synthesis, characterization and anticancer activity of vincristine loaded folic acid-chitosan conjugated nanoparticles on NCI-H460 non-small cell lung cancer cell line. Egyptian Journal of Basic and Applied Sciences 5 (1), 87–99.

Lei, S., Zheng, R., Zhang, S., Wang, S., Chen, R., Sun, K., et al., 2021. Global patterns of breast cancer incidence and mortality: A population-based cancer registry data analysis from 2000 to 2020. Cancer Commun. 41 (11), 1183–1194.

Li, H., Prever, L., Hirsch, E., Gulluni, F., 2021. Targeting PI3K/AKT/mTOR signaling pathway in breast cancer. Cancers 13 (14), 3517.

Loerzel, V. W. 2015. Symptom experience in older adults undergoing treatment for cancer. Number 3/May 2015, 42(3), E269-E278.

Mani, S., Balasubramanian, B., Balasubramani, R., Chang, S.W., Ponnusamy, P., Esmail, G.A., et al., 2020. Synthesis and characterization of proanthocyanidin-chitosan nanoparticles: An assessment on human colorectal carcinoma HT-29 cells. J. Photochem. Photobiol. B Biol. 210, 111966.

Naahidi, S., Jafari, M., Edalat, F., Raymond, K., Khademhosseini, A., Chen, P., 2013. Biocompatibility of engineered nanoparticles for drug delivery. J. Control. Release 166 (2), 182–194.

Patnaik, A., Appleman, L.J., Mountz, J.M., Ramanathan, R.K., Beeram, M., Tolcher, A. W., et al., 2011. A first-in-human phase I study of intravenous PI3K inhibitor BAY 80–6946 in patients with advanced solid tumors: Results of dose-escalation phase. J. Clin. Oncol. 29 (15), 3035.

Pijuan, J., Barceló, C., Moreno, D.F., Maiques, O., Sisó, P., Marti, R.M., et al., 2019. In vitro cell migration, invasion, and adhesion assays: from cell imaging to data analysis. Front. Cell Dev. Biol. 7, 107.

Pompura, S.L., Dominguez-Villar, M., 2018. The PI3K/AKT signaling pathway in regulatory T-cell development, stability, and function. J. Leukoc. Biol. 103 (6), 1065–1076.

Prasad, M., Salar, A., Salar, R.K., 2022. In vitro anticancer activity of curcumin loaded chitosan nanoparticles (CLCNPs) against Vero cells. Pharmacological Research-Modern Chinese Medicine 3, 100116.

Rehman, S., Ashfaq, U.A., Riaz, S., Javed, T., Riazuddin, S., 2011. Antiviral activity of Acacia nilotica against Hepatitis C Virus in liver infected cells. Virol. J. 8, 1–6.

Rozana, R., Yulizar, Y., Saefumillah, A., & Apriandanu, D. O. B. 2020. Synthesis, characterization and in vitro release study of efavirenz-loaded chitosan nanoparticle. In AIP Conference Proceedings (Vol. 2242, No. 1, p. 040004). AIP Publishing LLC.

Sakhi, M., Khan, A., Iqbal, Z., Khan, I., Raza, A., Ullah, A., et al., 2022. Design and characterization of paclitaxel-loaded polymeric nanoparticles decorated with trastuzumab for the effective treatment of breast cancer. Front. Pharmacol. 13.

Sandhiutami, N.M.D., Arozal, W., Louisa, M., Rahmat, D., Wuyung, P.E., 2021. Curcumin nanoparticle enhances the anticancer effect of cisplatin by inhibiting PI3K/AKT and JAK/STAT3 pathway in rat ovarian carcinoma induced by DMBA. Front. Pharmacol. 11, 603235.

Sartaj, A., Qamar, Z., Qizilbash, F.F., Md, S., Alhakamy, N.A., Baboota, S., Ali, J., 2021. Polymeric nanoparticles: exploring the current drug development and

therapeutic insight of breast cancer treatment and recommendations. Polymers 13 (24), 4400.

Sarwar, M.R., Saqib, A., 2017. Cancer prevalence, incidence and mortality rates in Pakistan in 2012. Cogent Medicine 4, (1) 1288773.

Shafqat, O., Rehman, Z., Shah, M.M., Ali, S.H.B., Jabeen, Z., Rehman, S., 2023. Synthesis, structural characterization and in vitro pharmacological properties of betanin-encapsulated chitosan nanoparticles. Chem. Biol. Interact. 370, 110291.

Shen, Y., Xiao, Y., Zhang, S., Wu, S., Gao, L., Shi, S., 2020. Fe3O4 nanoparticles attenuated Salmonella infection in chicken liver through reactive oxygen and autophagy via PI3K/Akt/mTOR signaling. Front. Physiol. 10, 1580.

Shetake, N.G., Kumar, A., Gaikwad, S., Ray, P., Desai, S., Ningthoujam, R.S., et al., 2015. Magnetic nanoparticle-mediated hyperthermia therapy induces tumour growth inhibition by apoptosis and Hsp90/AKT modulation. Int. J. Hyperth. 31 (8), 909–919.

Stuelten, C.H., Barbul, A., Busch, J.I., Sutton, E., Katz, R., Sato, M., et al., 2008. Acute wounds accelerate tumorigenesis by a T cell–dependent mechanism. Cancer Res. 68 (18), 7278–7282.

Subramaniyan, S., Kamaraj, Y., Kumaresan, V., Kannaiyan, M., David, E., Ranganathan, B., et al., 2022. Green synthesized zinc oxide nanoparticles induce apoptosis by suppressing PI3K/Akt/mTOR signaling pathway in osteosarcoma MG63 cells. Global Translational Medicine 1 (1), 1–12.

Sundaram, G.M., Ismail, H.M., Bashir, M., Muhuri, M., Vaz, C., Nama, S., et al., 2017. EGF hijacks miR-198/FSTL1 wound-healing switch and steers a two-pronged pathway toward metastasis. J. Exp. Med. 214 (10), 2889–2900.

Sung, H., Ferlay, J., Siegel, R.L., Laversanne, M., Soerjomataram, I., Jemal, A., Bray, F., 2021. Global cancer statistics 2020: GLOBOCAN estimates of incidence and mortality worldwide for 36 cancers in 185 countries. CA Cancer J. Clin. 71 (3), 209–249.

Tran, P., Lee, S.E., Kim, D.H., Pyo, Y.C., Park, J.S., 2020. Recent advances of nanotechnology for the delivery of anticancer drugs for breast cancer treatment. J. Pharm. Investig. 50, 261–270.

Udayakumar, G.P., Muthusamy, S., Selvaganesh, B., Sivarajasekar, N., Rambabu, K., Banat, F., et al., 2021. Biopolymers and composites: Properties, characterization and their applications in food, medical and pharmaceutical industries. J. Environ. Chem. Eng. 9, (4) 105322.

Vij, M., Calderaro, J., 2021. Pathologic and molecular features of hepatocellular carcinoma: an update. World J. Hepatol. 13 (4), 393.

Wang, W., Tong, C.Y., Liu, X.Y., Li, T., Liu, B., Xiong, W., 2015. Preparation and functional characterization of tumor-targeted folic acid-chitosan conjugated nanoparticles loaded with mitoxantrone. J. Cent. South Univ. 22 (9), 3311–3317.

Wu, J., Shu, Q., Niu, Y., Jiao, Y., Chen, Q., 2018. Preparation, characterization, and antibacterial effects of chitosan nanoparticles embedded with essential oils synthesized in an ionic liquid containing system. J. Agric. Food Chem. 66 (27), 7006–7014.

Wu, C., Zhu, Y., Wu, T., Wang, L., Yuan, Y.I., Chen, J., et al., 2019. Enhanced functional properties of biopolymer film incorporated with curcurmin-loaded mesoporous silica nanoparticles for food packaging. Food Chem. 288, 139–145.

Xiong, K., Zhang, Y., Wen, Q., Luo, J., Lu, Y., Wu, Z., et al., 2020. Co-delivery of paclitaxel and curcumin by biodegradable polymeric nanoparticles for breast cancer chemotherapy. Int. J. Pharm. 589, 119875.

Xu, J., Lai, H., You, L., Zhao, Z., 2022. Improvement of the stability and anti-AGEs ability of betanin through its encapsulation by chitosan-TPP coated quaternary ammonium-functionalized mesoporous silica nanoparticles. Int. J. Biol. Macromol. 222, 1388–1399.

Yip, P.Y., 2015. Phosphatidylinositol 3-kinase-AKT-mammalian target of rapamycin (PI3K-Akt-mTOR) signaling pathway in non-small cell lung cancer. Translational lung cancer research 4 (2), 165.

Zhu, S., Yao, F., Li, W.H., Wan, J.N., Zhang, Y.M., Tang, Z., et al., 2013. PKCδ-dependent activation of the ubiquitin proteasome system is responsible for high glucose-induced human breast cancer MCF-7 cell proliferation, migration and invasion. Asian Pac. J. Cancer Prev. 14 (10), 5687–5692.